Void growth in metal anodes in solid-state batteries: recent progress and gaps in understanding

S.S. Shishvan[a,b], N.A. Fleck[a], R.M. McMeeking[c] and V.S. Deshpande[a*]

[a] *Department of Engineering, University of Cambridge, Cambridge CB2 1PZ, UK*
[b] *Department of Structural Engineering, University of Tabriz, Tabriz, Iran*
[c] *Department of Mechanical Engineering & Materials Department, University of California, Santa Barbara CA 93106, USA*

Abstract

Stripping of metal cations from the anode of a Li- or Na-ion cell into a ceramic electrolyte results in the formation of voids on the electrolyte/electrode interface. Such voids have been observed to grow to sizes in excess of 100 μm. Dendrites can nucleate and grow in the electrolyte from the vicinity of the voids during the plating phase of cycling of the cell, and lead to short-circuiting of the cell. Current theoretical understanding of the formation of these voids is in its infancy: the prevailing qualitative notion is that voids form within the metal anode when the stripping current density removes metal from the interface faster than it can be replenished. We review models that employ the Onsager formalism to develop a variational approach to model void growth by coupling power-law creep of the metal electrode and the flux of metal cations through a single-ion conductor solid electrolyte. These models, based on standard Butler-Volmer kinetics for the interfacial flux, predict that voids will shrink for realistic combinations of interfacial ionic resistance and electrolyte conductivity. Additional physics in the form of modified kinetics, such that the interfacial resistance is decreased by the presence of dislocations within the creeping metal electrode, are shown to give rise to initial growth of voids around impurity particles on the electrolyte/electrode interface. However, these voids ultimately collapse under the imposed stripping fluxes and no conditions have been identified for which isolated voids grow to more than 10 μm in size. This is in contrast to the experimentally observed sizes of ~100 μm. The physical processes by which large voids form remain unclear but the current state-of-the-art understanding does provide clues of possible mechanisms that have not as yet been considered.

Keywords: Solid-state battery, ceramic electrolyte, Butler-Volmer kinetics, void growth

* Corresponding author. E-mail address: vsd20@cam.ac.uk

1. Introduction

Ceramic electrolytes show promise for widespread use in Lithium (Li) and Sodium (Na) ion batteries. Upon combining with Li or Na metal anodes they have the potential to deliver higher energy densities with enhanced safety compared to liquid electrolyte batteries (Takada, 2013; Wang et al., 2021). However, upon charging such cells at current densities greater than a critical value, fissures commonly termed as "dendrites" nucleate and grow from the metal electrode and result in short-circuiting the cell. Dendrites can adopt a range of morphologies from planar filaments that involve fracture of the ceramic electrolyte to a 3D 'mossy' form that is thought to originate from the filling of interconnected porosity. Several aspects of this failure mechanism are established through the recent work of Bruce and co-workers (Kazemchainan et al., 2019, Jolly et al., 2020), and Sakamoto and co-workers (Schmidt and Sakamoto, 2016; Kazyak et al., 2020; Chang et al., 2021). These include the fact that the critical current required to short-circuit the cell increases with decreasing interfacial ionic resistance to the flux of metal ions across the electrolyte/electrode interface (Sharafi et al., 2017a) and that, unlike dendrites in liquid electrolytes, cracks in solid electrolytes are only partially filled with metal (Hao et al., 2020; Ning et al., 2021).

Bruce and co-workers (Kazemchainan et al., 2019; Jolly et al., 2020) have suggested that there are two relevant critical current densities: the critical current on stripping (CCS) that results in void formation at the electrolyte/electrode interface, and the critical current on plating (CCP) at which dendrites grow into the ceramic electrolyte from the plating metal electrode. Typically, CCS is less than CCP and it has been shown both experimentally (Kazemchainan et al., 2019; Raj et al. 2022) and via recent theoretical predictions (Shishvan et al., 2020a, b) that Li filaments preferentially grow from the vicinity of the voids at the electrolyte/electrode interfaces. Thus, an understanding of the mechanics of void growth at the electrolyte/electrode interface is essential to address the dendrite problem. Void growth in Li electrodes have been experimentally observed at interfaces with both LLZO ($Li_7La_3Zr_2O_{12}$) (Krauskopf et al., 2019a; Wang et al., 2019) and Argyrodite (Li_6PS_5Cl) electrolytes (Kazemchainan et al., 2019; Lu et al., 2022); see Fig. 1a. Similarly, interfacial void formation has been reported for Na/Na-β''-alumina/Na cells (Jolly et al., 2020); see Fig. 1b. For the Li/LLZO system, void growth, or rather the formation of instabilities at the interface, was observed at currents as low as 0.1 mA cm^{-2} when no stack pressure was applied (Krauskopf et al., 2019a). Application of a stack pressure increased the CCS for both the Li/Argyrodite (Kazemchainan et al., 2019) and Li/LLZO (Wang et al., 2019) systems. After cycling at 1.0 mA cm^{-2} to an areal capacity 1 mA h cm^{-2}, voids of size > 100 μm typically form (Kazemchainan et al., 2019) though the size of these voids at initiation is typically less than 1 μm (Lu et al., 2022). Changing the composition of the Li electrode by alloying with 10 at.% Mg (Krauskopf et al., 2019b) has been suggested as a route to reduce the propensity for void formation.

Recent observations have shown that cell failure due to void formation is not only dependent upon the stripping current but also on the stripping time and electrode thickness (Lee et al., 2022). These observations suggest that the mechanics governing the formation and growth of voids in the metal electrode is a complex combination of (i) the electrochemical kinetics of the electrolyte/electrode interface and (ii) creep/plastic deformation and vacancy diffusion within the metal electrode as well as along the surface/interface. While some simplistic models (Krauskopf et al., 2019a; Wang et al., 2019; Chen et al., 2020; Zhang et al., 2020; Yan et al., 2021; Lu et al., 2022) suggest that vacancy diffusion plays a dominant role, some other models (Shishvan et al., 2021; Roy et al., 2021; Agier et al., 2022) suggest an alternative mechanism of void growth by flux focussing. Despite intensive research, a fundamental understanding of the mechanism of void growth has remained elusive.

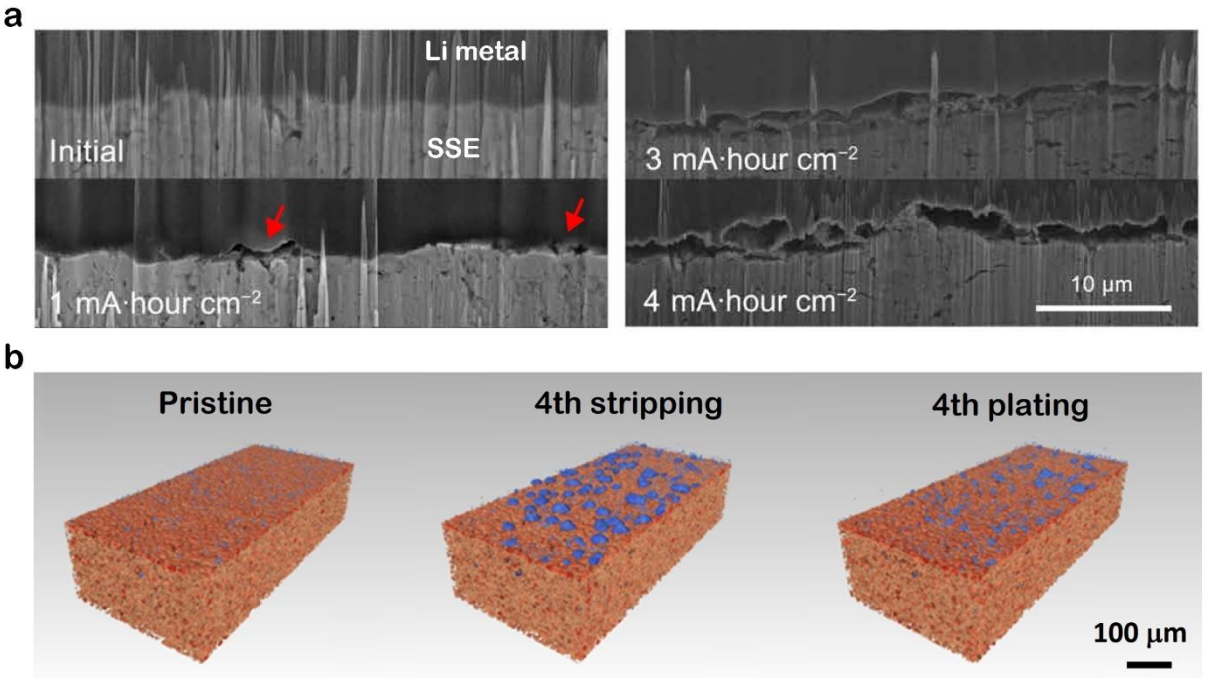

Figure 1: (a) Cross-sectional SEM images of the LPS electrolyte/Li electrode interface during continuous Li stripping at a current density of 0.5 mA cm^{-2} showing void initiation and growth. Adapted from Lu et al. (2022). (b) X-ray tomography images of the Na/Na-β″-alumina cell interfaces when pristine and after the 4th stripping and the 4th plating showing that voids only partially close on plating. Blue indicates voids in the Na metal anode (transparent) and orange indicates the solid electrolyte. The cell was cycled at a current density of 1.5 mA cm^{-2}. Adapted from Jolly et al. (2020).

The aim of this article is primarily to present a broad overview of the mechanisms proposed for void growth in metal electrodes during stripping and thereby demonstrate the gaps on our understanding. In Section 2, we first provide a critical overview of the two main void growth mechanisms proposed in the literature and thereby argue that the flux focussing mechanism is most plausible. However, the flux focussing models presented to-date neglect diffusion along the electrolyte/electrode interface and we therefore extend the model of Agier et al. (2022) in Section 3 to account for this mechanism. Critically, we show that including interface diffusion is unlikely to change the flux focussing predictions presented to-date. Therefore, in Section 4 we focus on numerical results mainly from the existing literature to reveal the state-of-the-art. These predictions illustrate the limitations of the current models to explain experimental observations. Finally in Section 5, possible directions of future investigations are outlined in order to close the gap between models and observations. While the formulation and qualitative results are applicable to both Na- and Li-ion cells, we shall give results only for Li-ion cells as they have been the focus of the literature.

2. A critical review of two commonly proposed mechanisms of void growth

Two mechanisms have been most commonly proposed in the literature for void formation at the electrolyte/electrode interface:

(i) Void formation and growth by vacancy generation and coalescence at the electrolyte/electrode interface (Fig. 2a).

(ii) Void growth due to flux focussing at the periphery of initial imperfections on the electrolyte/electrode interface (Fig. 3a).

Both mechanisms are based on the notion that the metal is stripped from the electrode at the interface faster than it is replenished. We shall briefly discuss both mechanisms and their inherent shortcomings.

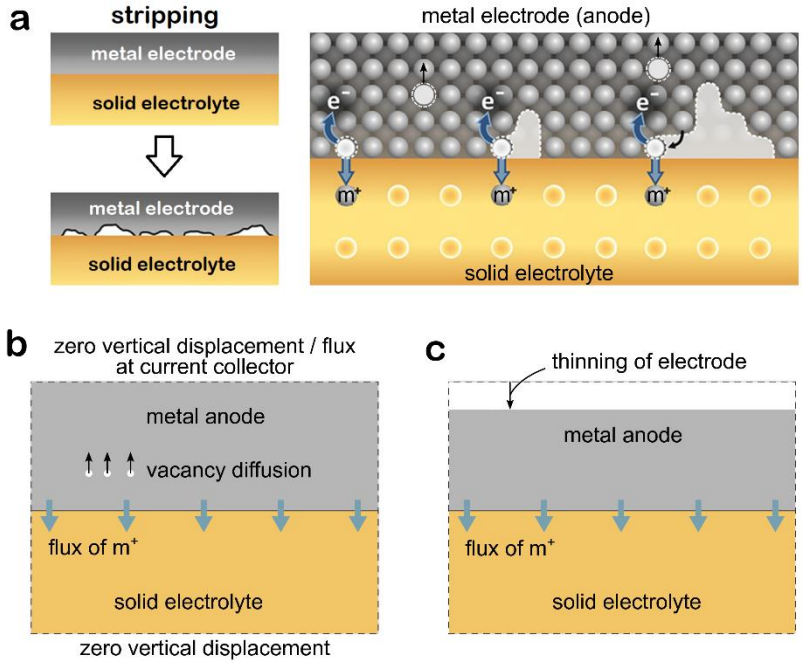

Figure 2: (a) Sketch illustrating the mechanism of void formation at the electrolyte/electrode interface by vacancy generation and coalescence during stripping of metal ions (m^+). Vacancies are generated at the interface during stripping and their diffusion away from the interface is slower than the rate at which metal atoms are stripped. (b) Sketch of the boundary value problem solved (see for example Yan et al., 2021) to model this mechanism. (c) The thinning of the electrode by drift or rigid body motion is illustrated here. The analysis shown in (b) neglects this drift by fixing the current collector end of the electrode.

First, consider the mechanism of void formation via vacancy generation and coalescence. The basic idea is that as metal ions (m^+) are stripped from the electrode at the interface, vacancies are generated (Fig. 2a) and these vacancies then diffuse into the electrode thereby replenishing the interface with metal atoms. If the stripping fluxes exceed the rate at which the metal atoms can be replenished by vacancy diffusion, vacancies accumulate and coalesce at the interface resulting in void formation and growth (see Fig. 2a). Several calculations have been reported to quantify this assumed mechanism (Krauskopf et al., 2019a; Yan et al., 2021; Zhao et al. 2022; Lu et al., 2022). While there are a few differences in the details of these calculations, the boundary value problem that is solved in all cases is essentially the same and is sketched in Fig. 2b. Importantly, a zero displacement or equivalently zero flux boundary condition is imposed on the current collector end of the electrode. As a consequence, the overall electrode volume remains unchanged and, as the metal is stripped from the electrode, the electrode becomes increasingly porous. In reality, stripping of the metal from the electrolyte/electrode interface results in drift or rigid body motion of the electrode (Fig. 2c) with the electrode losing metal (and volume). The convective motion of lithium in the electrode compensates for the stripping at the interface and there is minimal or no vacancy generation or flux within the electrode due to the stripping current. Translation of the electrode is also consistent with the observation that the metal electrode thins upon stripping. Thus, void generation as predicted

by these models is an artifact of the assumption of an unrealistic boundary condition[1]. This is also clear from thermodynamic perspective. Vacancies in Li have a large enthalpy of formation of approximately 50 kJ mol^{-1} making large concentrations of vacancies highly unfavourable (coalescence of vacancies is even more unfavourable as the enthalpies of di- and tri-vacancies are in excess of 100 kJ mol^{-1}). While diffusion is slow and may not be able to annihilate vacancies formed by stripping, there is no such speed restriction on drift which acts to prevent the electrode from attaining a very highly unfavourable thermodynamic state.

A recent investigation by Lewis et al. (2023) has attempted to account for drift of the electrode using a phase-field formulation. This study predicts some void growth after stripping of nearly the full electrode but void growth in the majority of the literature occurs much earlier; see for example Kazemchainan et al. (2019). While the reasons for this discrepancy are unclear, it could be due to two reasons: (i) in Lewis et al. (2023) the authors impose a spatially constant drift velocity at the current collector end which essentially makes the numerical problem ill-posed and (ii) they use an unrealistic interface resistance of zero but employing a Dirichlet boundary condition at the electrolyte/electrode interface. Nonetheless the study shows that the literature is recognising the need to account for the drift of the electrode.

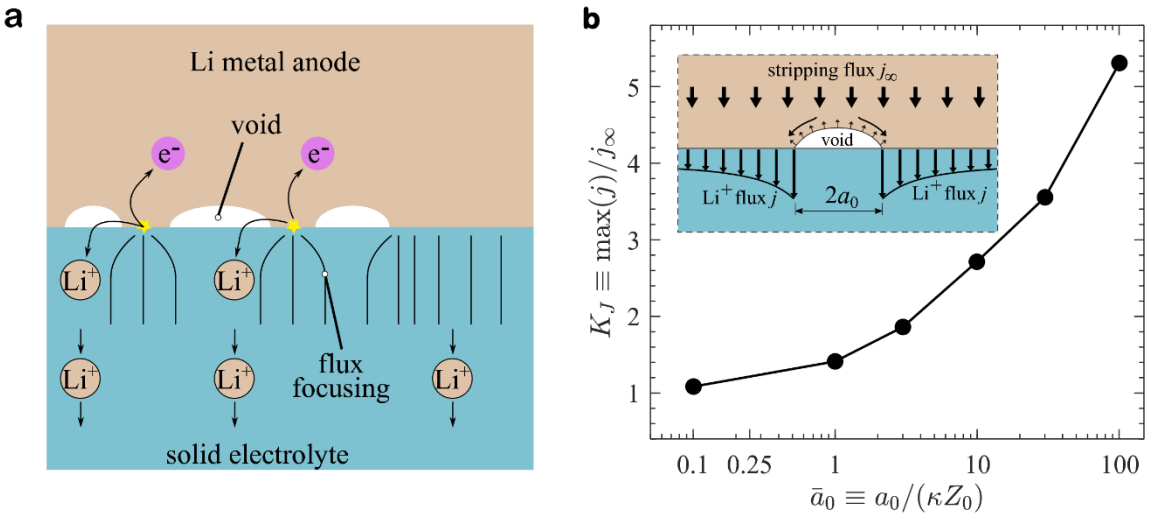

Figure 3: (a) Sketch illustrating the idea of flux focussing at the periphery of initial imperfections on the electrolyte/electrode interface. (b) Predictions of the flux focussing factor K_J around the periphery of the imperfection as a function of the normalised imperfection size $\bar{a}_0 \equiv a_0/(\kappa Z_0)$ using standard Butler-Volmer kinetics; adapted from Roy et al. (2021). The inset shows the problem analysed with a pre-existing void of diameter $2a_0$ at the interface. Flux focussing tends to sweep the Li metal over the void surface via diffusion/creep and grow the void while the drift of the electrode due to the stripping flux tends to close the void.

Second, consider the alternative mechanism of void growth by flux focussing. There is a large literature (see Roy et al. (2021) and references therein) that assumes that focusing of the ionic flux occurs at the periphery of initial imperfections on the electrolyte/electrode interface, and the flux focussing drives void initiation and growth (Fig. 3a). The basic hypothesis is shown in the inset of Fig. 3b and is explained as follows. Loss of contact between the electrolyte and the electrode due to surface roughness (Fig. 3a) and/or imperfections along the interface give rise

[1] A common, everyday example to illustrate this point is the grating of cheese. As the cheese is grated, fresh cheese arrives by translation of the residual block of cheese. The effect of grating does not make the cheese block porous.

to regions over the electrolyte/electrode interface where flux of the metallic cations is blocked. These regions are idealised as circular disks of diameter $2a_0$ in the inset of Fig. 3b. The resulting spatially inhomogeneous electric field within the electrolyte focuses the flux around the periphery of the imperfection. This flux focussing results in growth of the void due to the creep deformation of electrode. However, Roy et al. (2021) has addressed that this simple explanation, based on Butler-Volmer kinetics for the interfacial flux, has a flaw as summarized here. The ratio of maximum interfacial flux at the periphery of the imperfection, $\max(j)$, to the far-field interfacial flux j_∞ is defined as the flux focussing factor K_J. Figure 3b replots the predictions of Roy et al. (2021) of K_J as a function of $\bar{a}_0 \equiv a_0/(\kappa Z_0)$ using the usual Butler-Volmer kinetics; here, Z_0 is the interfacial resistance and κ is the ionic conductivity of the electrolyte. We note that a material length scale is defined by the product κZ_0 and this length scale for typical Li-ion cells is $\kappa Z_0 \approx 20$ μm (using $\kappa = 0.4$ mS cm^{-1} and $Z_0 = 5\ \Omega$ cm^2 as reported by Sharafi et al. (2017b)). The predictions of Roy et al. (2021) suggest that the flux focussing factor K_J is < 3 for $\bar{a}_0 < 10$ (Fig. 3b) and consequently this analysis suggests that flux focussing is small for imperfections of size $a_0 < 200$ μm. Roy et al. (2021) considered in detail the case of $\kappa Z_0 = 20$ μm, and predicted that no void growth will occur from imperfections less than 1 mm in size (and initial interfacial imperfections > 1 mm are unrealistically large)[2]. They comment that convection of the electrode due to the stripping flux tends to close the voids and overpowers the effect of flux focussing. While voids do grow to > 100 μm in size (Kazemchainan et al., 2019; Lu et al., 2022), they typically have sub-micron sizes in the early stages of growth (Lu et al., 2022).

Shishvan et al. (2021) have argued that flux focussing must occur, and the insufficient flux focussing seen in Fig. 3b is because standard Butler-Volmer kinetics are inappropriate for an electrode that deforms by power-law creep. Recall that Butler-Volmer kinetics, as employed in most of the literature, including the work of Roy et al. (2021), assumes that the electrode is not deforming. This implies spatially uniform stripping/plating over the interface with the metal electrode maintaining full contact with a rigid ceramic electrolyte. But void growth is accompanied by power-law creep deformation of the metal electrode and associated non-uniform stripping of the electrode. Recall that climb-mediated glide of dislocations is the mechanics of power-law creep (Sargent and Ashby, 1984). The consequent nucleation and multiplication of dislocations that accompanies power-law creep reduces the interfacial resistance which in turn enhances flux focussing (Shishvan et al., 2021). Consequently, void growth can initiate from sub-micron impurity particles. The work of Shishvan et al. (2021) has recently been extended to predict the growth of voids within Li metal electrodes (Agier et al., 2022).

3. Analysis of void growth in the metal electrode

We consider the axisymmetric problem shown in Fig. 4, with the interface between electrode and electrolyte defined as $z = 0$. Cations of Li^+ are stripped from the electrode by an ionic flux across the electrolyte/electrode interface. The presence of a void or impurity particle on the interface eliminates the flux over a small region on the interface. We envision that this inhomogeneity in interfacial flux results in the growth of a void in the Li electrode at the electrolyte/electrode interface. This problem has recently been analysed by Agier et al. (2022) but they neglected the effect of diffusion along the electrolyte/electrode interface that is often cited as being an important mechanism to drive void growth. Thus, here we extend the

[2] A corollary to this prediction is that atomic scale inhomogeneities caused by the formation of vacancies during stripping will also result in negligible flux focussing.

variational principle developed by Agier et al. (2022) to include the effect of interface diffusion on void growth by using the Onsager (1931a, b) formalism for non-equilibrium processes. We shall show that the usual form of linearized Butler-Volmer interfacial flux relation holds in the presence of a void growing within the creeping electrode with interface diffusion also present.

We model the initial interface heterogeneity as either a hemispherical void, or a small hemispherical impurity particle, of radius a_0 such that flux across the interface over a circular area of radius a_0 is prevented. While contact between the Li electrode and the rigid ceramic electrolyte is maintained, the growth of the void involves creep deformation of the Li electrode as well as diffusion of Li along the electrolyte/electrode interface.

3.1 Variational principle for interfacial flux

Consider the symmetric cell as shown in Fig. 4a that comprises two Li electrodes and the electrolyte. We focus on the Li anode that is subjected to a stack pressure p_0 and is maintained at a uniform electric potential ϕ_p. We analyse a spatially fixed portion of the Li cell as sketched in Fig. 4b: within this portion is a spatially fixed volume V of the electrode (Fig. 4c). The volume V is assumed to be large and deformation of the Li primarily occurs within a local volume (indicated by hatched marking in Fig. 4c) at the location where void growth may occur near the electrolyte/electrode interface. A region $V_\mathrm{Li} \leq V$ is occupied by the Li in V with the remainder occupied by the impurity and/or void (Fig. 4d). We use the symbol S to denote the surface of V with S_m denoting the top surface and S_I denoting the bottom surface along the electrolyte/electrode surface at $z = 0^-$ (Fig. 4c). Note that the bottom surface of V and V_Li do not coincide with the bottom surface of V_Li denoted by S_b (Fig. 4d). We partition S_b into two portions such that $S_\mathrm{b} \equiv S_\mathrm{e} \cup S_\mathrm{v}$ with S_e being along $z = 0^-$ where the Li is in contact with the electrolyte (i.e., S_e is common to S_b and S_I) and S_v is the impurity particle surface or void surface. (If the Li is in contact with the impurity, S_v is the impurity particle surface while it is the traction-free void surface if the Li is detached from the impurity.) Note that while S_e and S_v are not spatially fixed boundaries during the void growth, the top and lateral boundaries of V_Li are spatially fixed. Thus, the region V_Li (Fig. 4d) is a mixed Lagrangian/Eulerian domain. Since the region V (Fig. 4c) is a spatially fixed region, it is convenient to define V as the system in developing a variational principle and consider the rate of potential energy change and dissipation within this system.

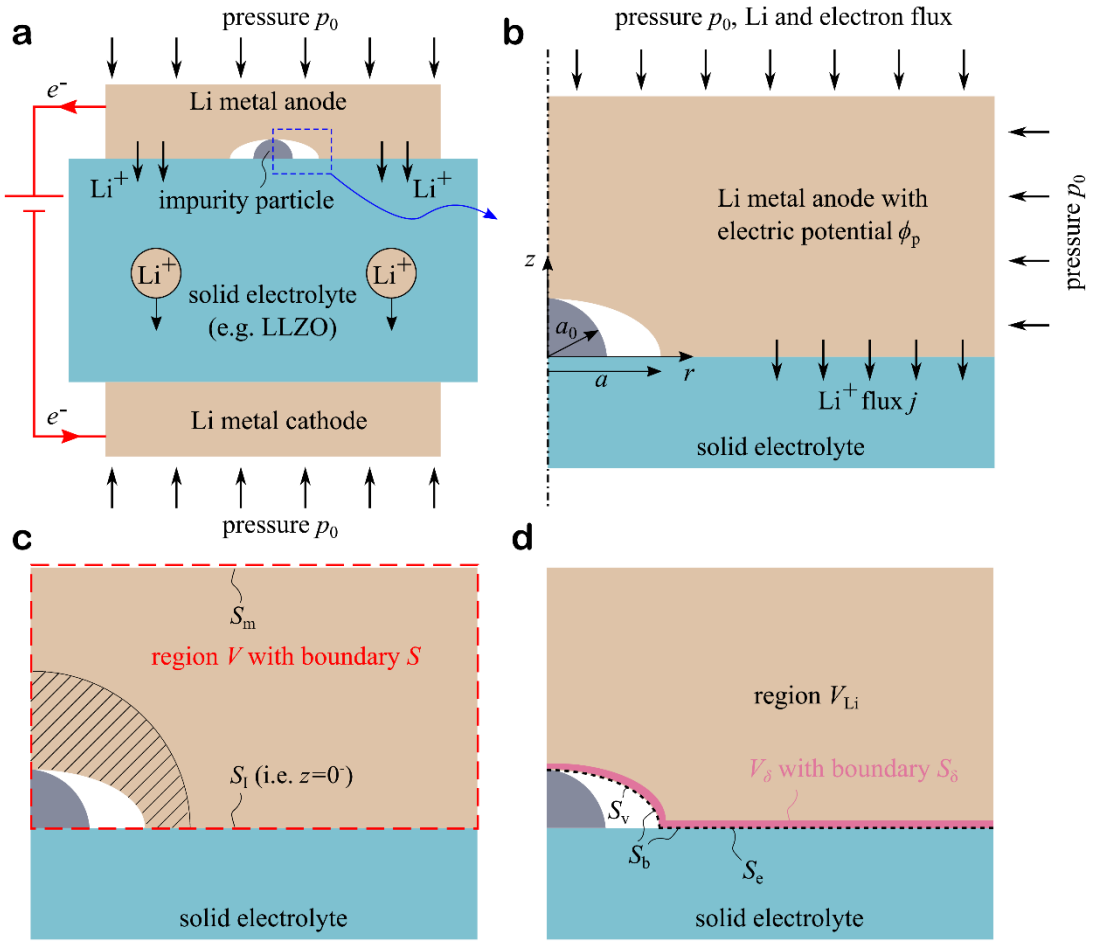

Figure 4: (a) Sketch of the axisymmetric problem with an isolated hemispherical void/impurity on the interface of the solid electrolyte/stripping electrode. An external power source maintains an electrical potential difference between the electrodes of the symmetric cell. (b) Zoom-in of the small region that is analysed and shown by the dashed rectangular box in (a). The (r, z) co-ordinate system is included with the electrolyte/electrode interface along $z = 0$. (c) Sketch to show the system V (dashed red line), and its upper and lower boundaries S_m and S_I, respectively. Deformation of the Li primarily occurs within a local volume as indicated by hatched marking. (d) The volume V_Li that the Li occupies within V. The lower boundary of V_Li is $S_\mathrm{b} \equiv S_\mathrm{e} \cup S_\mathrm{v}$ as depicted by the dashed black line. The pink region is the interface region V_δ (with boundary S_δ) over which diffusion of Li occurs.

The Onsager formalism requires that the kinetic path followed by the system is such that arbitrary variations in rate kinematic degrees of freedom give a rate of change of potential energy that is balanced by the variation in the dissipation rate. First consider the rate of change of potential energy $\dot{\Pi}$ within the system. While the stack pressure p_0 and Li flux on the top surface S_m of V are spatially uniform and normal to the surface, the Li fluxes across the lateral boundaries of V vanish. With μ_0 denoting the reference chemical potential of Li, the chemical potential of the Li in V is $\mu_\mathrm{Li} = \mu_0 + p\Omega_\mathrm{Li}$, where Ω_Li is the molar volume of Li and the pressure p can vary spatially within V. Thus, $\mu_\mathrm{Li} = \mu_0 + p_0\Omega_\mathrm{Li}$ represents the chemical potential of Li entering V via the top surface S_m. The Li ions in the electrolyte (with the reference chemical potential μ_0^e) cause neither swelling nor shrinkage of the single ion conductor electrolyte and the concentration of Li^+ within the electrolyte balances the fixed and uniform distribution of anions in order to maintain electroneutrality. Thus, along the portion S_e of the bottom surface of V, the chemical potential of Li^+ exiting the system is $\mu_{Li^+}^\mathrm{e} = \mu_0^\mathrm{e} + F\phi$, where F is the Faraday constant and ϕ is the electric potential in the electrolyte evaluated at the interface. Assuming (i) isothermal conditions for the volume V and (ii) an equilibrium vacancy

concentration, the rate of change of the Helmholtz free energy of V is $\dot{A} = \dot{N}_{\mathrm{Li}}\mu_0$, where the rate of change of Li molar content N_{Li} in V is denoted by $\dot{N}_{\mathrm{Li}}$. Write the chemical potential of the electrons within the electrode as $\mu_{\mathrm{el}^-} = -F\phi_{\mathrm{p}}$. For an isothermal process, the second law of thermodynamics requires that the rate of change of potential energy $\dot{\Pi}$ for the volume V satisfies the inequality

$$\dot{\Pi} \equiv \dot{A} + \int_{S_{\mathrm{m}}} \mu_{\mathrm{Li}} f_i^{\mathrm{Li}} n_i dS - \frac{1}{F}\int_{S_{\mathrm{m}}} \mu_{\mathrm{el}^-} j_i^{\mathrm{el}^-} n_i dS + \frac{1}{F}\int_{S_{\mathrm{e}}} \mu_{\mathrm{Li}^+}^{\mathrm{e}} j_i^{\mathrm{Li}^+} n_i dS \leq 0, \tag{1}$$

where f_i^{Li} is the molar flux of Li, $j_i^{\mathrm{el}^-}$ is the current density vector accounting for the flux of electrons across S_{m}, $j_i^{\mathrm{Li}^+}$ is the current density vector accounting for the Li^+ flux across S_{e} (upon noting that the only flux leaving V over S_{I} is across S_{e}) and n_i denotes the outward unit normal to the respective surfaces.

The volume V remains charge neutral so as conservation of charge requires

$$\int_{S_{\mathrm{m}}} j_i^{\mathrm{el}^-} n_i dS + \int_{S_{\mathrm{e}}} j_i^{\mathrm{Li}^+} n_i dS = 0, \tag{2}$$

while conservation of Li demands

$$\int_{S_{\mathrm{m}}} f_i^{\mathrm{Li}} n_i dS + \frac{1}{F}\int_{S_{\mathrm{e}}} j_i^{\mathrm{Li}^+} n_i dS = -\dot{N}_{\mathrm{Li}}\,. \tag{3}$$

Upon substituting for the chemical potentials, viz. $\mu_{\mathrm{Li}^+}^{\mathrm{e}} = \mu_0^{\mathrm{e}} + F\phi$, $\mu_{\mathrm{el}^-} = -F\phi_{\mathrm{p}}$ and $\mu_{\mathrm{Li}} = \mu_0 + p\Omega_{\mathrm{Li}}$, as well as recalling that $p = p_0$ is spatially uniform over S_{m}, it follows from (3) that the rate of change of potential energy $\dot{\Pi}$ given by (1) can be rephrased as

$$\dot{\Pi} = \frac{1}{F}\int_{S_{\mathrm{e}}} (\mu_0^{\mathrm{e}} - \mu_0 + F\phi) j_i^{\mathrm{Li}^+} n_i dS + \phi_{\mathrm{p}}\int_{S_{\mathrm{m}}} j_i^{\mathrm{el}^-} n_i dS + p_0\Omega_{\mathrm{Li}}\int_{S_{\mathrm{m}}} f_i^{\mathrm{Li}} n_i dS. \tag{4}$$

With the open circuit potential given by $\mathcal{U} \equiv (\mu_0^{\mathrm{e}} - \mu_0)/F$, the overpotential across the electrolyte/electrode interface is defined as $\eta \equiv \phi_{\mathrm{p}} - (\phi + \mathcal{U})$. Now make use of (2) to give

$$\dot{\Pi} = -\int_{S_{\mathrm{e}}} \eta j_i^{\mathrm{Li}^+} n_i dS + p_0\Omega_{\mathrm{Li}}\int_{S_{\mathrm{m}}} f_i^{\mathrm{Li}} n_i dS. \tag{5}$$

The decrease in $\dot{\Pi}$ is associated with the following dissipation mechanisms in V: (i) dissipation by creep of the bulk electrode; (ii) dissipation by diffusion of Li along S_{b} and (iii) dissipation associated with the flux of Li^+ across the electrolyte/electrode interface. Consider each of these dissipation mechanisms in turn. First, dissipation in the bulk of the Li electrode is due to incompressible creep flow of the Li, driven by the deviatoric stress $s_{ij} \equiv \sigma_{ij} - (\sigma_{kk}/3)\delta_{ij}$, where σ_{ij} is stress and δ_{ij} is the usual Kronecker delta symbol. A dissipation potential Φ_{m} is introduced in terms of the incompressible creep strain rate $\dot{\varepsilon}_{ij}^{\mathrm{C}}$, such that

$$s_{ij} \equiv \frac{\partial \Phi_{\mathrm{m}}}{\partial \dot{\varepsilon}_{ij}^{\mathrm{C}}}. \tag{6}$$

The dissipation rate per unit volume in the bulk electrode is directly related to Φ_{m} by $\dot{d}_{\mathrm{m}} = (\partial\Phi_{\mathrm{m}}/\partial\dot{\varepsilon}_{ij}^{\mathrm{C}})\dot{\varepsilon}_{ij}^{\mathrm{C}}$. Note that $\Phi_{\mathrm{m}} = 0$ in the void and/or impurity particle.

Second, consider surface/interfacial dissipation within a thin strip on the electrode side of the boundary $S_{\mathrm{b}} \equiv S_{\mathrm{e}} \cup S_{\mathrm{v}}$. The strip is an inter-phase rather than an interface and has a thickness δ of atomic dimension in which diffusional flow of Li plays a significant role. Denote the volume of this thin strip by V_δ and its entire boundary by S_δ (Fig. 4d) and note that V_δ is

bounded on one side by S_b as already stated. The volumetric flux q_i of Li in V_δ is given by (Needleman and Rice, 1980)

$$q_i = -m\frac{\partial \mu_{\mathrm{Li}}}{\partial x_i} = -m\Omega_{\mathrm{Li}}\frac{\partial p}{\partial x_i}, \tag{7}$$

where m is the mobility of Li in V_δ (note that $m \to 0$ outside V_δ). Upon writing a dissipation potential associated with this linear diffusion process as

$$\Phi_\mathrm{D} \equiv \frac{1}{2}\frac{q_i q_i}{m\Omega_{\mathrm{Li}}}, \tag{8}$$

the dissipation rate is given by $\dot{d}_\mathrm{D} = (\partial\Phi_\mathrm{D}/\partial q_i)q_i$.

Third, following Shishvan et al. (2021), define an electrolyte/electrode interface dissipation potential $\Phi_\mathrm{I} \equiv j^2 Z/2$ (where $j = j_i^{\mathrm{Li}^+} n_i$ and n_i, the unit normal to S_e, points into the electrolyte) in terms the interfacial resistance Z which in general need not be spatially uniform. The dissipation rate per unit area of the interface is then $\dot{d}_\mathrm{I} = j(\partial\Phi_\mathrm{I}/\partial j)$.

To proceed with the variational principle, introduce the functional

$$\Psi\left(\dot{\varepsilon}_{ij}^\mathrm{C}, q_i, j_i^{\mathrm{Li}^+}\right) \equiv \dot{\Pi} + \int_{S_\mathrm{e}} \Phi_\mathrm{I} dS + \int_V \Phi_\mathrm{m} dV + \int_{V_\delta} \Phi_\mathrm{D} dV, \tag{9}$$

with the kinematic solution satisfying $\delta\Psi = 0$. Upon substituting for the various terms in (9), we write the variation of Ψ as

$$\begin{aligned} \delta\Psi = &-\int_{S_\mathrm{e}} \eta\delta j_i^{\mathrm{Li}^+} n_i dS + p_0\Omega_{\mathrm{Li}}\int_{S_\mathrm{m}} \delta f_i^{\mathrm{Li}} n_i dS \\ &+ \int_{S_\mathrm{e}} \frac{\partial\Phi_\mathrm{I}}{\partial j}\delta j_i^{\mathrm{Li}^+} n_i dS + \int_{V_{\mathrm{Li}}} \frac{\partial\Phi_\mathrm{m}}{\partial\dot{\varepsilon}_{ij}^\mathrm{C}}\delta\dot{\varepsilon}_{ij}^\mathrm{C} dV + \int_{V_\delta} \frac{\partial\Phi_\mathrm{D}}{\partial q_i}\delta q_i dV \\ &= \delta\dot{\Pi} + \int_{S_\mathrm{e}} \delta\dot{d}_\mathrm{I}\, dS + \int_{V_{\mathrm{Li}}} \delta\dot{d}_\mathrm{m}\, dV + \int_{V_\delta} \delta\dot{d}_\mathrm{D}\, dV, \end{aligned} \tag{10}$$

where $\delta\dot{d}_\mathrm{m} = s_{ij}\delta\dot{\varepsilon}_{ij}^\mathrm{C} = \sigma_{ij}\delta\dot{\varepsilon}_{ij}^\mathrm{C}$ since $\dot{\varepsilon}_{kk}^\mathrm{C} = 0$ and $\Phi_\mathrm{m} = 0$ in the void and/or impurity particle and therefore we have replaced the integral over V by the integral over V_{Li}.

The term associated with diffusional dissipation can be rephrased as

$$\int_{V_\delta} \frac{\partial\Phi_\mathrm{D}}{\partial q_i}\delta q_i dV = -\int_{V_\delta} \frac{\partial p}{\partial x_i}\delta q_i dV = -\int_{V_\delta} p\delta\dot{\varepsilon}_\mathrm{D} dV - \int_{S_\delta} p n_i \delta q_i dS, \tag{11}$$

where the volumetric strain rate $\dot{\varepsilon}_\mathrm{D}$ satisfies $\dot{\varepsilon}_\mathrm{D} = -q_{i,i}$. The normal flux $q_i n_i = 0$ over all portions of S_δ by the following arguments:

(i) Symmetry requires that $q_i n_i = 0$ along the left boundary of S_δ

(ii) Along the right boundary of S_δ also $q_i n_i$ vanishes since Li does not leave the domain along that boundary.

(iii) Over the top surface of S_δ the diffusive flux normal to S_δ vanishes since $m = 0$ in the bulk of V_{Li}.

(iv) The flux again vanishes across the bottom surface S_δ (i.e., S_b) as there is no diffusive flux neither across the void surface S_v nor across the electrolyte/electrode interface S_e.

Thus,

$$\int_{V_\delta} \frac{\partial\Phi_\mathrm{D}}{\partial q_i}\delta q_i dV = -\int_{V_\delta} p\delta\dot{\varepsilon}_\mathrm{D} dV, \tag{12}$$

and it follows that

$$\int_{V_{\mathrm{Li}}} \frac{\partial \Phi_{\mathrm{m}}}{\partial \dot{\varepsilon}_{ij}^{\mathrm{C}}} \delta \dot{\varepsilon}_{ij}^{\mathrm{C}} dV + \int_{V_\delta} \frac{\partial \Phi_{\mathrm{D}}}{\partial q_i} \delta q_i dV = \int_{V_{\mathrm{Li}}} \sigma_{ij} \delta \dot{\varepsilon}_{ij} dV, \tag{13}$$

where the total strain rate is related to the material velocity of the Li in the electrode via $\dot{\varepsilon}_{ij} = 0.5(v_{i,j} + v_{j,i})$ such that $\dot{\varepsilon}_{ij} = \dot{\varepsilon}_{ij}^{\mathrm{C}}$ at a location x_i in $V_{\mathrm{Li}} \notin V_\delta$ and $\dot{\varepsilon}_{ij} = \dot{\varepsilon}_{ij}^{\mathrm{C}} + \delta_{ij}\dot{\varepsilon}_{\mathrm{D}}/3$ for x_i in V_δ. Then, application of the stress equilibrium relation $\sigma_{ij,j} = 0$ along with the divergence theorem implies

$$\int_{V_{\mathrm{Li}}} \frac{\partial \Phi_{\mathrm{m}}}{\partial \dot{\varepsilon}_{ij}^{\mathrm{C}}} \delta \dot{\varepsilon}_{ij}^{\mathrm{C}} dV + \int_{V_\delta} \frac{\partial \Phi_{\mathrm{D}}}{\partial q_i} \delta q_i dV = \int_{S_{\mathrm{m}}} T_i \delta v_i dS + \int_{S_{\mathrm{b}}} T_i \delta v_i dS. \tag{14}$$

Now recall that if the Li is detached from the impurity, the traction T_i vanishes and if it remains in contact with the impurity particle, the normal velocity $v_i n_i = 0$. Moreover, we assume that over both the impurity particle and the electrolyte surface S_{e} the Li is free to slip such that $T_i t_i = 0$ with t_i as a unit vector along the interface S_{e}. Then (14) reduces to

$$\int_{V_{\mathrm{Li}}} \frac{\partial \Phi_{\mathrm{m}}}{\partial \dot{\varepsilon}_{ij}^{\mathrm{C}}} \delta \dot{\varepsilon}_{ij}^{\mathrm{C}} dV + \int_{V_\delta} \frac{\partial \Phi_{\mathrm{D}}}{\partial q_i} \delta q_i dV = -p_0 \int_{S_{\mathrm{m}}} n_i \delta v_i dS + \int_{S_{\mathrm{e}}} T_n \delta v_n dS, \tag{15}$$

where $T_n = T_i n_i$ on S_{e} and $T_i = -p_0 \delta_{ij} n_j$ on S_{m} while $v_n = v_i n_i$. Now substitute (15) into (10) and set $\delta\Psi = 0$ to obtain

$$\int_{S_{\mathrm{e}}} \eta \delta j dS - \int_{S_{\mathrm{e}}} Z j \delta j dS = \frac{\Omega_{\mathrm{Li}}}{F} \int_{S_{\mathrm{e}}} T_n \delta j dS, \tag{16}$$

where we have used the continuity relation $v_i = j_i^{\mathrm{Li}^+} \Omega_{\mathrm{Li}}/F$ over S_{e} and an equivalent result on S_{m} along with the definition $\Phi_{\mathrm{I}} \equiv j^2 Z/2$. Then, upon noting that this relation holds for arbitrary variations δj, it follows that

$$j = \frac{\eta - T_n \Omega_{\mathrm{Li}}/F}{Z}. \tag{17}$$

The usual form of the linearized Butler-Volmer relation (see e.g., Monroe and Newman, 2005; Ahmad and Viswanathan, 2017; Barai et al., 2018; Mistry and Mukherjee, 2020) is thus reproduced but here we have shown that it applies for an electrode wherein deformation occurs by creep and diffusional flow might occur along the electrolyte/electrode interface. We note in passing that the stress (or traction) term in (17) is significantly smaller that the overpotential η and plays a negligible role for all realistic stripping currents as quantified by Shishvan et al. (2021).

In the above treatment, we have assumed that the surface and interface energies of the lithium are negligible and set them to zero. As a consequence, surface curvature plays no role in driving diffusion at the boundary of the Lithium. Additionally, diffusional flux along the electrolyte/electrode interface does not affect the Butler-Volmer relation (17), and thus it is reasonable to assume that diffusional flux along the electrolyte/electrode interface will have a negligible influence on void growth. Roy et al. (2021) had reached a similar conclusion based on the argument that diffusional flow rates due to interface traction/pressure gradients are significantly slower than the fluxes due to the imposed electrical potential. Thus, in the remainder of this article we shall discuss numerical results where creep of the electrode is considered but diffusion along the electrolyte/electrode interface is neglected. Nevertheless, the formulation Eq. (1) to Eq. (17) has successfully incorporated surface and interface Li

diffusion and is being exploited in current research to explore the effects of surface and interface Li diffusion.

3.2 Predictions of void growth during stripping

Agier et al. (2022) predicted void growth during stripping of Li from a Li electrode into a LLZO electrolyte. Here we focus on summarising the key physical understanding from this study. All results are presented in terms of an imposed nominal cell current j_∞ per unit electrolyte/electrode interface area. We shall first consider the case where the interface kinetics is described by standard Butler-Volmer kinetics with an interfacial resistance $Z = Z_0 = 5\ \Omega\ \mathrm{cm}^2$ that is taken to be spatially uniform and not dependent on the deformation of the electrode. The electrolyte is assumed to be LLZO of ionic conductivity $\kappa = 0.46\ \mathrm{mS\ cm}^{-1}$; see Agier et al. (2022) for further details of the calculations including all material parameters.

Envision that a pre-existing hemispherical void of radius $a_0 = 0.25\ \mu\mathrm{m}$ resides within the Li electrode, with its diametral base plane on the electrolyte/electrode interface. Predictions of the temporal evolution of the void for an imposed stripping current $j_\infty = 0.5\ \mathrm{mA\ cm}^{-2}$ are shown in Fig. 5 (where the time $t = 0$ corresponds to the instant that j_∞ is first imposed). In contrast to observations that stripping results in void growth (Kazemchainan et al., 2019; Lu et al., 2022), void shrinkage is predicted. A qualitative explanation for the mechanisms of void growth/shrinkage has already been given in Section 2 but we reiterate it here with further details. Stripping results in flux focussing on the periphery of the initial void as sketched in the inset of Fig. 3b. The enhanced flux at the void periphery (due to this flux focussing) is thought to draw Li from the surface of the void thereby growing the void as sketched in the inset of Fig. 3b. However, what is commonly ignored is the fact that the overall imposed stripping flux results in the drift of the electrode towards the electrolyte (with the drift velocity of $j_\infty \Omega_{\mathrm{Li}}/F$) and this tends to close the void (inset of Fig. 3b). Thus, void growth will only occur if the flux focussing is sufficiently high to overcome the effect of the overall stripping/drift current closing the void.

The simulations presented in Fig. 5 include contours of normalized flux j_z/j_∞ in the electrolyte (here j_z is the flux in the electrolyte in the z −direction) as well as contours of von Mises stress σ in the Li electrode normalised by the reference strength $\sigma_0 = 1$ MPa of the Li. The stress state within the electrode is vanishingly small indicating negligible straining within the electrode and suggesting that the electrode is stripping via pure drift (that is, rigid body motion). To further illustrate this, contours of the Stokes stream function ψ within the Li electrode are included. These surfaces represent a constant difference in value of the stream function, i.e., $\Delta\bar{\psi} \equiv \Delta\psi F/(j_\infty \Omega_{\mathrm{Li}} a_0^2) = 0.5$ for this case, so that the volumetric flow rate of the Li between consecutive surfaces equals $Q = 2\pi\Delta\psi = \pi a_0^2 j_\infty \Omega_{\mathrm{Li}}/F$. The contours are almost vertical. Recalling that the stream function contours are parallel to the material velocities, this further confirms that void shrinkage occurs with Li being uniformly stripped over the electrolyte/electrode interface S_{e}. (Note that the contours of j_z in the electrolyte also shown in Fig. 5 confirm that there is no/minimal flux focussing.) Thus, these coupled simulations clearly show that the flux focussing mechanism based on standard Butler-Volmer kinetics is insufficient to induce void growth, as previously suggested by the decoupled simulations of Roy et al. (2021).

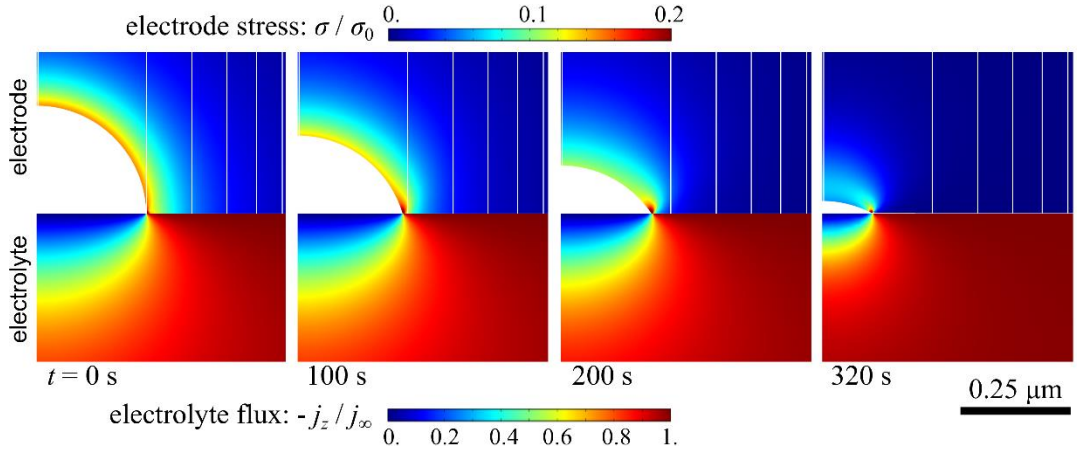

Figure 5: Snapshots showing the temporal evolution of a hemispherical void of radius $a_0 = 0.25$ μm within the electrode on the electrolyte/electrode interface. These predictions with a stripping current $j_\infty = 0.5$ mA cm^{-2} employ standard Butler-Volmer kinetics with an interfacial resistance $Z = Z_0 = 5\ \Omega\ \text{cm}^2$. Contours of the normalised flux j_z/j_∞ in the electrolyte and the von-Mises stress σ/σ_0 in the Li are included. To indicate the flow of the Li and the associated velocity gradients, we superimpose contour surfaces $\bar{\psi}$ of equally spaced Stokes stream functions (with $\Delta\bar{\psi} = 0.5$).

4. Effect of creep deformation on interfacial resistance

Butler-Volmer kinetics provides a relation for the flux across the electrolyte/electrode interface as a function of voltage jump when the electrode is not deforming. This assumption is valid when plating/stripping of Li is spatially uniform over the interface. Void growth is associated with spatially non-uniform stripping and is consequently accompanied by creep deformation of the electrode. In these circumstances, Shishvan et al. (2021) hypothesized that key assumptions in deriving standard Butler-Volmer kinetics are violated and that the interfacial resistance Z, instead of being constant, depends on the rate of deformation (creep) of the Li electrode. Here, we first summarize their hypothesis and then discuss the consequences. The presence of a finite stack pressure p_0 will contribute to void collapse and so in the following discussion and analysis we shall continue to consider the case where no stack pressure is applied as we are primarily concerned with understanding the growth of voids.

Creep deformation of the Li electrode under deviatoric stress is by the motion of dislocations with the dislocation density depending upon the level of deviatoric stress (Weertman, 1968; Sargent and Ashby, 1984). Shishvan et al. (2021) argued that dislocations influence interface kinetics in two ways:

(i) Dislocations cause a small expansion of the metal lattice and this in turn increases the effective vacant space within the Li electrode. The effective fraction, $\hat{\theta}_\text{v}$, of vacant lattice sites is related to the density ρ_d of dislocations of Burgers vector b via

$$\hat{\theta}_\text{v} = \exp\left(-\frac{h_\text{v}}{RT}\right) + \alpha\frac{\Omega_\text{Li}(\rho_\text{d} b^2)}{\Omega_\text{v}}, \tag{18}$$

where h_v is the enthalpy of vacancy formation in Li, Ω_v the molar volume of vacancies and α is a constant that depends on the metal crystal structure. For example, $\alpha \approx 0.25$ for fcc Cu and ≈ 2.7 for bcc Fe (Seeger and Haasen, 1958). The two terms in (18) are the fraction of vacancies at a temperature T in the Li (first term) and the second term that models the extra space due to expansion of the lattice by dislocations.

(ii) The elastic distortion of the lattice due to the dislocations that enhances the enthalpy of the Li atoms.

The Butler-Volmer assumption that the barrier is set by the weighted mean of the standard chemical potentials of the two end-states requires that the enthalpy and entropy of the electrode are known. Shishvan et al. (2021) assumed that $\hat{\theta}_{\mathrm{v}}$ is such that it minimizes the free-energy (i.e., an equilibrium assumption) and this enabled them to calculate the enthalpy and entropy of the electrode as a function of the dislocation density and thereby evaluate the interfacial barrier for Li ions to cross the electrolyte/electrode interface. This weighted barrier is shown schematically in Fig. 6 and illustrates that an increase in the standard chemical potential of the electrode Li ions due to the presence of dislocations reduces the barrier for the crossing of Li ions from the electrode to the electrolyte. We emphasize here that consistent with the conventional creep theory, the dislocation density does not change the free-energy and therefore the chemical potential of Li. Rather, the enthalpy (or standard chemical potential) increases, and this is balanced out by a corresponding increase in the configurational entropy to keep the chemical potential unchanged in the presence of the dislocations.

Shishvan et al. (2021) estimated the barrier illustrated in Fig. 6 and their analysis predicted that the interfacial resistance Z is related to the resistance Z_0 in the absence of dislocations via

$$Z = Z_0 \hat{\theta}_{\mathrm{v}}^{\ \beta-1} \exp\left[-\frac{(1-\beta)h_{\mathrm{v}}}{RT}\right]. \tag{19}$$

Here $0 \leq \beta \leq 1$ is the Butler-Volmer symmetry factor which is typically $\beta = 0.5$. Combining (18) and (19) it is clear that the interfacial resistance Z decreases with increasing dislocation density ρ_{d}. Recalling that the dislocation density in a creeping metal such as Li scales with the applied stress σ as $\rho_{\mathrm{d}} \propto (1/b^2)(\sigma/G_{\mathrm{Li}})$, where G_{Li} is the shear modulus of Li (Weertman, 1968), it follows that increasing the creep strain-rate (or equivalently increasing the stress) reduces the interfacial resistance in the vicinity of the imperfection. This thereby increases the flux focussing which in turn affects the creep of the electrode, resulting in a strong coupling between interface kinetics and creep deformation.

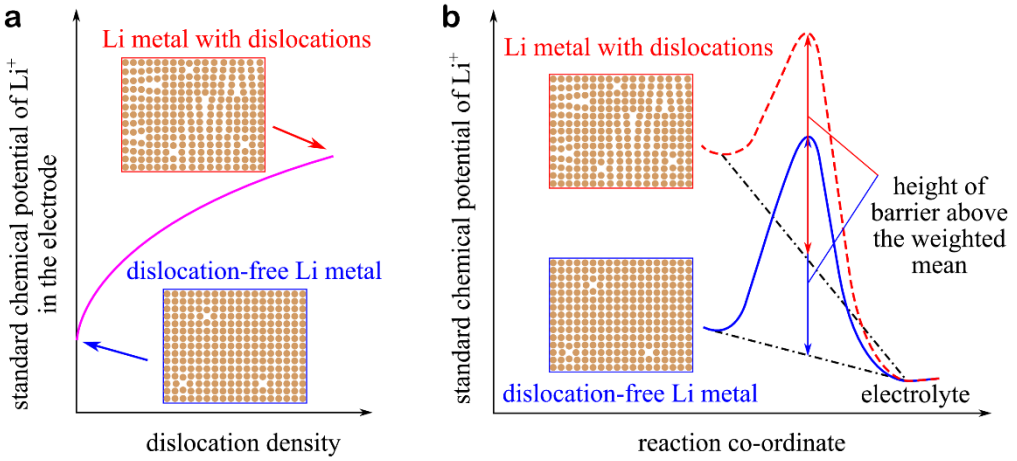

Figure 6: Schematics from Shishvan et al. (2021) to illustrate the effect of dislocations on the interfacial flux. (a) The enthalpy/standard chemical potential of the Li-ions increases with dislocation density in the electrode and (b) the energy landscape for an elementary Li-ion to transition from the electrode to the electrolyte. Curves are shown for the cases where the electrode is dislocation-free (solid blue) and where dislocations are present (dashed red).

4.1 Flux focussing with modified Butler-Volmer kinetics

Predictions of the normalised interfacial flux j/j_∞ as a function of the non-dimensional position r/a_0 along the interface at time $t = 0^+$ are included in Fig. 7a for three choices of the radius a_0 of the initial hemispherical void. Use of the modified Butler-Volmer kinetics also predicts

only a small flux focussing at the periphery of the void ($r/a_0 = 1$) with the flux dropping to its far-field value of j_∞ for $r/a_0 > 3$. These predictions are independent of j_∞ and, for realistic initial void sizes ($a_0 \leq 1$ μm), the voids again shrink. To understand why the modified Butler-Volmer kinetics does not change the results from Section 2.3, recall that stripping in the presence of a pre-existing void occurs by pure drift of the electrode without creep deformation. Therefore, there is no dislocation or stress generation within the Li electrode and $Z \approx Z_0$, i.e., the modified Butler-Volmer kinetics reduces to standard Butler-Volmer kinetics with negligible flux focussing and the shrink of voids of all realistic sizes.

When dislocations are present within the electrode, modified Butler-Volmer kinetics is expected to enhance flux focussing by reducing the interfacial resistance around the void/imperfection on the interface. However, generation of dislocations requires deformation, i.e., a spatially non-uniform velocity field. A spatially non-uniform velocity field is inevitable when an impurity particle is present on the interface as flux is prevented over a small patch of the interface and compatibility of deformation then means that Li flows over the impurity particle surface. This spatially inhomogeneous flow within the Li generates dislocations. We now proceed to consider the exemplar problem of a hemispherical solid impurity particle of radius a_0 on the interface, with modified Butler-Volmer kinetics.

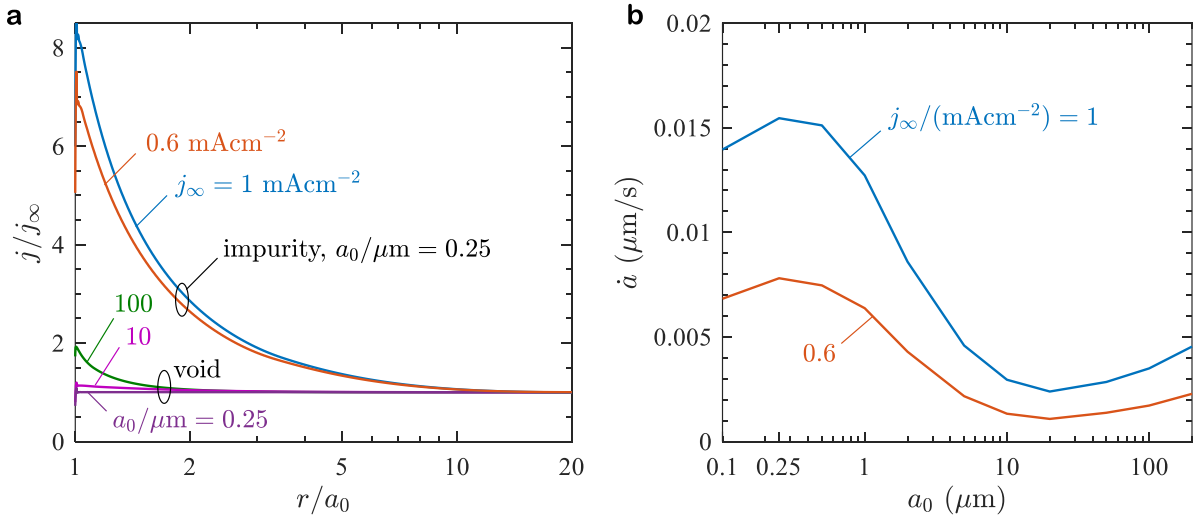

Figure 7: (a) The spatial variation of the normalised flux j/j_∞ over the interface at time $t = 0^+$ for the cases of hemispherical voids (three void radii a_0 are shown) and a hemispherical impurity of size $a_0 = 0.25$ μm at the interface. (b) The growth rate $\dot{a}$ of the void along the interface at time $t = 0^+$ as a function of the radius a_0 of the hemispherical impurity. Results are shown for two choices of the stripping current j_∞. Adapted from Agier et al. (2022) with predictions shown using the modified Butler-Volmer kinetics.

The normalised flux j/j_∞ over the interface at the instant $t = 0^+$ when the current is first imposed are included in Fig. 7a for $j_\infty = 1$ mA cm^{-2} and 0.6 mA cm^{-2} and impurity of radius $a_0 = 0.25$ μm. These results are in stark contrast to those for the pre-existing void: a flux focussing factor $K_J \approx 8.5$ is predicted for the impurity particle while $K_J \approx 1$ for the same size of a pre-existing void. Now recall that the low values of K_J associated with a pre-existing void (Fig. 7a) result in void shrinking over the full range of realistic void initial sizes; see for example Fig. 5. On the other hand, we expect the high K_J value around the impurity particle will initiate void growth. This was demonstrated by Agier et al. (2022) who showed that the initiation of void growth occurs at the periphery of the impurity along the electrolyte/electrode interface (i.e., at $(r, z) = (a_0, 0)$). Their predictions of the void growth rate $\dot{a}$ at $t = 0^+$ along $z = 0$ are included Fig. 7b as a function of the impurity radius a_0 for the two values of j_∞.

Note that a positive value of $\dot{a}$ implies the detachment of Li from the impurity along the electrolyte/electrode interface with the results in Fig. 7b indicating that voids initiate over the whole range of impurity particle sizes and current densities considered here. Moreover, the growth rate of $\dot{a}$ is sensitive to the value of K_J such that a higher K_J (at the higher value of j_∞; see Fig. 7a) results in a higher initial growth rate of a void.

4.2 Void growth around impurity particles

The calculations of Agier et al. (2022) demonstrated two distinct regimes of void growth around impurity particles that depend upon both the current and impurity size. We proceed to summarise these regimes by discussing results for a high and low stripping current j_∞ and an impurity of radius $a_0 = 0.25$ μm.

(a) *High stripping current.* Predictions of the temporal evolution of a void growing around the impurity with $j_\infty = 1$ mA cm^{-2} are shown in Fig. 8a, along with spatial distributions of the normalised von-Mises stress σ/σ_0 in the Li electrode and normalised flux j_z/j_∞ in the electrolyte. Surfaces of the Stokes stream function ψ (spaced at $\Delta\bar{\psi} \equiv \Delta\psi F/(j_\infty \Omega_{\mathrm{Li}} a_0^2) = 10$) are also included to illustrate the flow of Li within the electrode. The void growth is clearly divided into two phases. The void first grows along the electrolyte/electrode interface but without growing in height until $t \approx 400$ s. The contours ψ curve over the surface of this growing void consistent with the void growing in the $r-$direction. This results in a pancake-like shaped void consistent with experimental observations (Kazemchainan et al., 2019; Lu et al., 2022). Subsequently, for $t > 400$ s (and after the void has attained a radius $a \approx 4$ μm along the electrolyte/electrode interface) the void begins to collapse such that its height and volume reduces but its radius a remains approximately constant (Fig. 8a). We can understand this by recalling that the high flux focussing on the periphery of the void (as evident in the contours of j_z in Fig. 8a) causes the void to grow while simultaneously the overall stripping flux j_∞ (which induces a drift velocity of $j_\infty \Omega_{\mathrm{Li}}/F$ within the electrode) tends to close the void. When the void is small with respect to the impurity ($a/a_0 < 16$ in this case), the structural support of the impurity and the high flux focussing are together sufficient to cause the void to grow. However, for $a/a_0 \geq 16$, the support provided by the impurity is insufficient and the creep of the Li results in it beginning to collapse.

(b) *Low stripping current.* The temporal evolution of the Li around the impurity for the lower current of $j_\infty = 0.4$ mA cm^{-2} is illustrated in Fig. 8b in a manner analogous to Fig. 8a. A void again initiates from the surface of the impurity and grows along the interface resulting in a pancake-shaped void. However, the void now only attains a maximum radius $a \approx 1.5$ μm and more intriguingly this void stabilises at the state shown at $t = 1800$ s in Fig. 8b and does not collapse. The smaller growth is because the lower current implies a lower K_J and this limits the extent of void growth. Now the ratio of the void size to impurity size is lower and this implies more mechanical support from the impurity. In fact, in this case the flux focussing that tends to grow the void and the drift velocity of $j_\infty \Omega_{\mathrm{Li}}/F$ that tends to result in void collapse balance out. However, while voids in this case are stable, we emphasise they are much smaller than those observed in experiments (Kazemchainan et al., 2019; Lu et al., 2022).

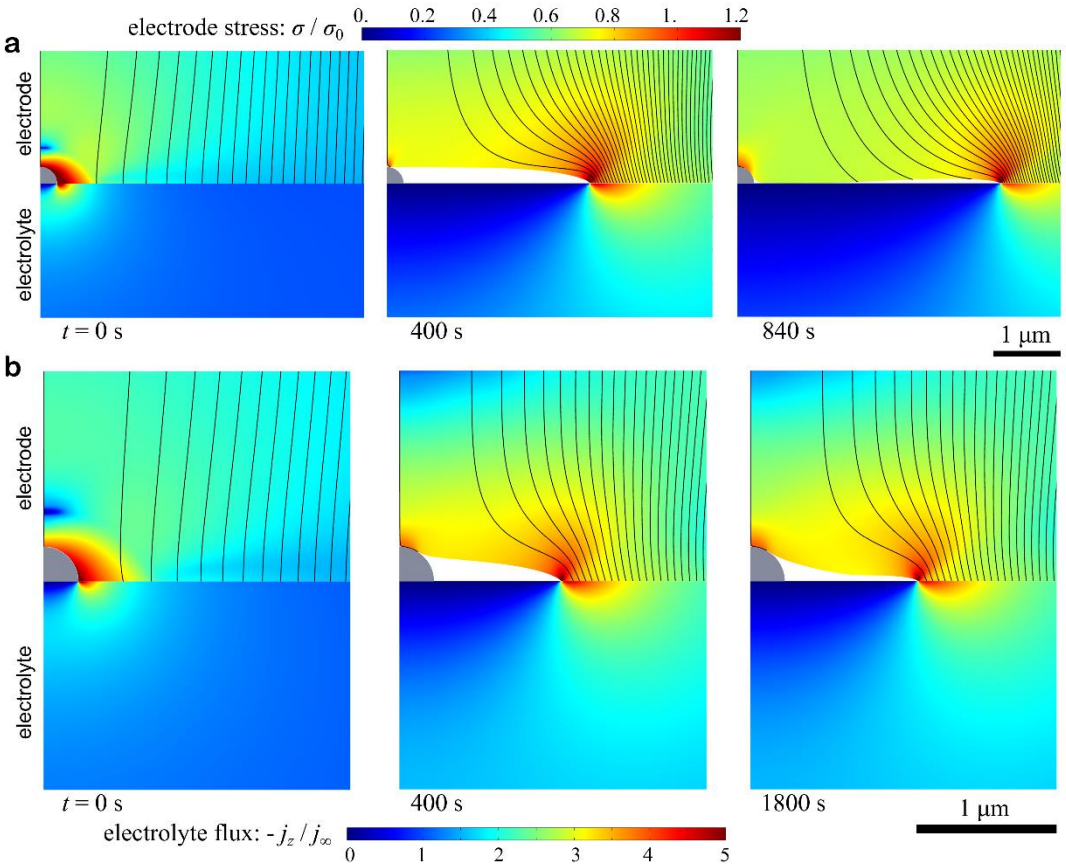

Figure 8: Predictions of the growth of a void around an $a_0 = 0.25$ μm impurity particle for the cases of stripping currents (a) $j_\infty = 1$ mA cm^{-2} and (b) $j_\infty = 0.4$ mA cm^{-2}. The results are shown using modified Butler-Volmer kinetics along with spatial distributions of the von-Mises stress σ/σ_0 in the Li and the flux j_z/j_∞ in the electrolyte. Contours of equally spaced Stokes stream functions (with $\Delta\bar{\psi} = 10$ for (a) and $\Delta\bar{\psi} = 4$ for (b)) are also included to indicate the flow of the Li and the associated velocity gradients. Adapted from Agier et al. (2022).

We define $a_{\max}$ as either the maximum radius of the stable void or the radius that the void attains before it begins to collapse. Predictions of $a_{\max} - a_0$ along the electrolyte/electrode interface as a function of j_∞ are summarised in Fig. 9a for calculations over a range of j_∞ and a_0 values. In Fig. 9a, the stable void cases are marked with filled symbols while an open symbol indicates that the void collapses. Whether the void is stable or collapses is dependent on both a_0 and j_∞ and the map in Fig. 9b summarises these regimes. Briefly, at low currents voids are stable but they collapse at higher currents with the current density at which the behaviour transitions between the two regimes increasing with increasing a_0.

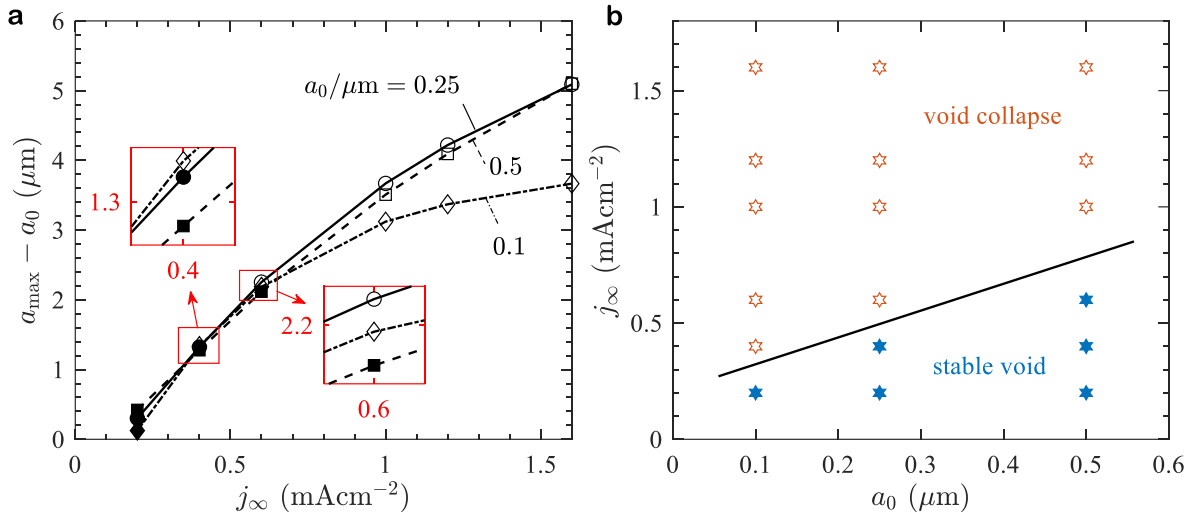

Figure 9: (a) Predictions of $a_{\max} - a_0$ along the electrolyte/electrode interface as a function of j_∞ for a void growing around an impurity particle of radius a_0. Here $a_{\max}$ is either the radius of the stable void or maximum radius of that the void attains before it collapses. The open and filled symbols indicate collapsing and stable voids, respectively. (b) A map using axes of a_0 and j_∞ summarises the two regimes, viz. void collapse and stable voids. The predictions are adapted from Agier et al. (2022) and use the modified Butler-Volmer kinetics.

5. Summary and need for further investigations

There now exists substantial experimental evidence that stripping of a metal anode in Li- or Na-ion cells with a ceramic electrolyte results in the formation of voids on the electrolyte/electrode interface. Two mechanisms have been proposed to explain this phenomenon:

(i) Void formation and growth by vacancy generation and coalescence at the electrolyte/electrode interface.

(ii) Void growth due to flux focussing at the periphery of initial imperfections on the electrolyte/electrode interface.

Both mechanisms are based on the idea that voids form because metal is stripped from the electrode at the interface faster than it is replenished. All models based on the notion that voids form due to vacancy generation and coalescence at the electrolyte/electrode interface have neglected the drift of the electrode that occurs during the stripping. This drift is directly observed in the form of thinning of the electrode; thereby, metal that is stripped from the electrode is replaced without the need for vacancy generation. Once electrode drift is properly accounted for in the models, the vacancy generation and coalescence mechanism will predict no void growth and can be discounted. We have therefore focussed our review on the flux focussing mechanisms.

A thermodynamically consistent numerical framework has been presented to predict the growth of voids at the electrolyte/electrode interface via a flux focussing mechanism. The framework employs the Onsager formalism to couple power-law creep deformation of the Li electrode, diffusion at the electrolyte/electrode interface and flux of Li^+ through a single-ion conductor solid electrolyte. Flux focussing, as predicted by standard Butler-Volmer interface kinetics, is negligible for all realistic sizes of initial voids on the electrolyte/electrode interface and consequently the stripping flux shrinks pre-existing voids. This is contrary to experimental

observations and suggests that it is necessary to revisit some of the key assumptions of the flux focussing mechanism. Some initial attempts in this direction are as follows.

Shishvan et al. (2021) have hypothesised that creep of the Li electrode associated with dislocation motion reduces the interfacial resistance and thereby enhances flux focussing. They developed a modified Butler-Volmer kinetics to include the effect of dislocation density within the electrode upon the interfacial resistance. However, stripping of an electrode with an initial void present on the electrolyte/electrode interface occurs with no deformation of the electrode. Since there is no creep within the electrode, the modified Butler-Volmer kinetics reduces to the standard case and the interfacial resistance is unaffected. Thus, again initial voids are predicted to shrink upon stripping of the electrode despite the assumption of modified Butler-Volmer kinetics. In contrast, an impurity on the electrolyte/electrode interface blocks interfacial Li flux and causes creep deformation of the electrode. In this case the modified Butler-Volmer kinetics predicts a significant flux focussing around the periphery of the impurity particle due to the high dislocation density associated with the creep of Li. This flux focussing induces growth of a void around the impurity particle. However, for realistic impurity particles sizes (i.e., on the order of a micron or less) voids no greater than 10 μm in size are predicted to form. This is significantly smaller than the experimentally observed voids which are on the order of 100 μm.

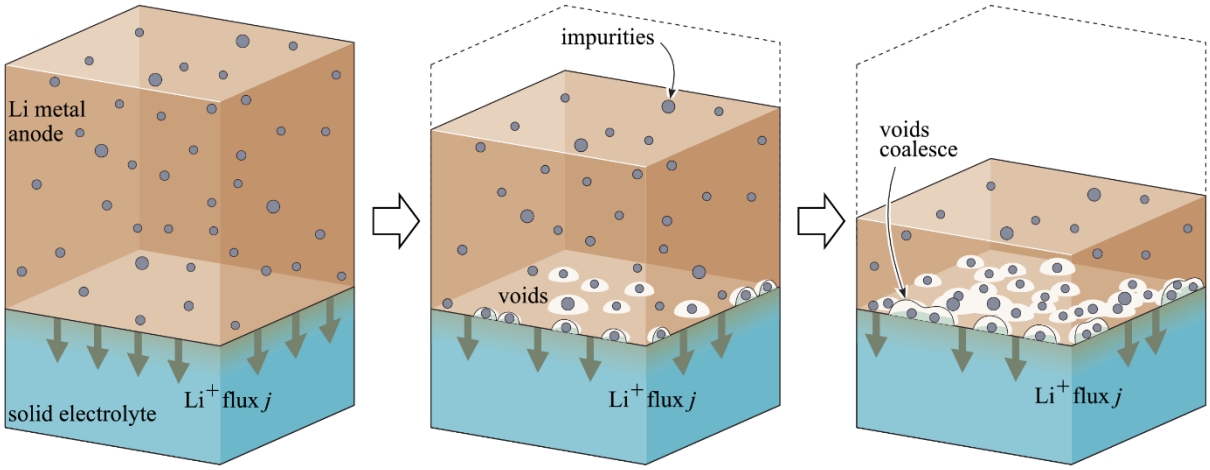

Figure 10: Sketches illustrating impurity particles dispersed in the Li electrode. These particles that are deposited on the electrolyte/electrode interface as Li is stripped from the electrode. Agier et al. (2022) hypothesized that the coalescence of voids that form around these deposited impurity particles can result in the formation of large voids with the impurity particles providing the structural support to prevent their collapse.

The underlying physics that promotes void growth to large sizes (e.g., > 100 μm) remains unclear. The model predictions discussed in Section 4 fulfil continuum balance laws and thermodynamic considerations but neglect atomic scale phenomena such as formation of Debye layers at the electrolyte/electrode interface. These charged layers are typically no more than 1 nm in thickness and their effect is accounted for in continuum models by parameters such as the interface resistance. The growth of voids on the order of few microns is expected to be largely governed by continuum balance laws and hence it is unlikely that neglecting the effect of these atomic scale effects of charged layers is a serious drawback of the current models in terms of predicting void growth. Nevertheless, the recent calculations summarised here suggest possible mechanisms that have been neglected in models developed to-date. In particular:

(i) The plastic/creep deformation of Li metal is size dependent with the strength of Li increasing when deformations are on the micron length scale (Xu et al., 2017). The enhanced micron-scale strength of Li metal might be sufficient to prevent the structural collapse of voids on the 100 μm length scale. Calculations using creep plasticity models (Geers et al., 2014) that allow for such plasticity size effects are needed to test this hypothesis.

(ii) Another possibility is the three-dimensional (3D) dispersion of impurity particles that are present inside a Li electrode and accumulate on the two-dimensional (2D) planar interface as stripping proceeds (Fig. 10). These impurities might provide structural support for the growing voids as sketched in Fig. 10 and thereby allowing for large voids to form by coalescence. This hypothesis implies that the total amount of Li that is stripped from the electrode governs void formation in addition to the stripping current. Agier et al. (2022) employed this hypothesis to suggest that the critical stripping capacity is given by[3]

$$C_{\mathrm{crit}} \approx \frac{F a_0^3}{4\Omega_{\mathrm{Li}} f a_{\mathrm{max}}^2}, \tag{20}$$

where f is the volume fraction of spherical impurity particles of radius a_0 dispersed within the stripping electrode. Recent experimental data (Lee et al., 2022) suggests that both stripping current and stripping time (or capacity) dictate failure by void formation at the electrolyte/electrode interface. While the critical capacity (20) predicted by Agier et al. (2022) is qualitatively consistent with these recent experimental findings, the use of a_{max} from Fig. 9a significantly overpredicts C_{crit} compared to the measurements. The combined effect of stack pressure, stripping capacity and current on the failure of solid-state Li-ion cells by void growth represents a rich area for future experimental and theoretical work.

References

Ahmad, Z., Viswanathan, V., 2017. Stability of Electrodeposition at Solid-Solid Interfaces and Implications for Metal Anodes. *Phys. Rev. Lett.* **119**, 056003.

Agier, J.A.B., Shishvan, S.S., Fleck, N.A., Deshpande, V.S., 2022. Void growth within Li electrodes in solid electrolyte cells. *Acta Mater.* **240**, 118303.

Barai, P., Higa, K., Srinivasan, V., 2018. Impact of External Pressure and Electrolyte Transport Properties on Lithium Dendrite Growth. *J. Electrochem. Soc.* **165**, A2654-A2666.

Chang, W., May, R., Wang, M., Thorsteinsson, G., Sakamoto, J., Marbella, L., Steingart, D., 2021. Evolving contact mechanics and microstructure formation dynamics of the lithium metal-Li7La3Zr2O12 interface. Nat. Commun. **12**, 6369.

Chen, Y., Wang, Z., Li, X., Yao, X., Wang, C., Li, Y., Xue, W., Yu, D., Kim, S.Y., Yang, F., Kushima, A., Zhang, G., Huang, H., Wu, N., Mai, Y.-W., Goodenough J.B., Li, J., 2020. Li metal deposition and stripping in a solid-state battery via Coble creep. *Nature* **578,** 251–255.

Geers, M.G.D., Cottura, M., Appolaire, B., Busso, E.P., Forest, S., Villani, A., 2014. Coupled glide-climb diffusion-enhanced crystal plasticity. *J. Mech. Phys. Solids* **70**, 136-153.

Jolly, D.S., Ning, Z., Darnbrough, J.E., Kasemchainan, J., Hartley, G.O., Adamson, P., Armstrong, D.E., Marrow, J., Bruce, P. G., 2020. Sodium/Na β" alumina interface: effect of pressure on voids. *ACS Appl. Mater. Interfaces* **12**, 678–685.

Kasemchainan, J., Zekoll, S., Jolly, D.S., Ning, Z., Hartley, G.O., Marrow, J., Bruce, P.G., 2019. Critical stripping current leads to dendrite formation on plating in lithium anode solid electrolyte cells. *Nat. Mater.* **18**, 1105-1111.

[3] There is a typographical error in the Agier et al. (2022) with Ω_{Li} missing in the denominator of this relation.

Krauskopf, T., Hartmann, H., Zeier, W.G., Janek, J., 2019a. Toward a fundamental understanding of the lithium metal anode in solid-state batteries - An electrochemo-mechanical study on the garnet-type solid electrolyte $Li_{6.25}Al_{0.25}La_3Zr_2O_{12}$. *ACS Appl. Mater. Interfaces* **11,** 14463–4477.

Krauskopf, T., Mogwitz, B., Rosenbach, C., Zeier, W.G., Janek, J., 2019b. Diffusion limitation of lithium metal and Li–Mg alloy anodes on LLZO type solid electrolytes as a function of temperature and pressure. *Adv. Eng. Mater.* **9**, 1902568.

Lee, K., Kazyak, E., Wang, M.J., Dasgupta, N.P., Sakamoto, J., 2022. Analyzing void formation and rewetting of thin in situ-formed Li anodes on LLZO. *Joule* **6**, 1–19.

Lewis, J.A., Sandoval, S.E., Liu, Y., Nelson, D.L., Yoon, S.G., Wang, R., Zhao, Y., Tian, M., Shevchenko, P., Martinez-Paneda, E., McDowell, M.T., 2023. Accelerated Short Circuiting in Anode-Free Solid-State Batteries Driven by Local Lithium Depletion. *Adv. Energy Mater.* 2204186

Lu, Y., Zhao, C.-Z., Hu, J.-K., Sun, S., Yuan, H., Fu, Z.-H., Chen, X., Huang, J.-Q., Ouyang, M., Zhang, Q., 2022. The void formation behaviors in working solid-state Li metal batteries. *Sci. Adv.* **8**, eadd0510.

Mistry, A., Mukherjee, P.P., 2020. Molar volume mismatch: A malefactor for irregular metallic electrodeposition with solid electrolytes. *J. Electrochem. Soc.* **167**, 082510.

Monroe, C., Newman, J., 2005. The impact of elastic deformation on deposition kinetics at lithium/Polymer Interfaces. *J. Electrochem. Soc.* **152**, A396-A404.

Needleman, A., Rice, J.R., 1980. Plastic creep flow effects in the diffusive cavitation of grain boundaries. *Acta Metall.* **28**, 1315–1332.

Ning, Z., Jolly, D.S., Li, G., De Meyere, R., Pu, S.D., Chen, Y., Kasemchainan, J., Ihli, J., Gong, C., Liu, B., Melvin, D.L.R., Bonnin, A., Magdysyuk, O., Adamson, P., Hartley, G.O., Monroe, C.W., Marrow, T.J., Bruce, P.G., 2021. Visualizing plating-induced cracking in lithium-anode solid-electrolyte cells. *Nat. Mater.* **20**, 1121-1129.

Onsager, L., 1931a. Reciprocal relations in irreversible processes, I. *Phys. Rev.* **37**, 405–426.

Onsager, L., 1931b. Reciprocal relations in irreversible processes, II. *Phys. Rev.* **38**, 2265–2279.

Raj, V., Venturi, V., Kankanallu, V.R., Kuiri, B., Viswanathan, V., Aetukuri, N.P.B., 2022. Direct correlation between void formation and lithium dendrite growth in solid-state electrolytes with interlayers. *Nat. Mater.* https://doi.org/10.1038/s41563-022-01264-8

Roy, U., Fleck, N.A., Deshpande, V.S., 2021. An assessment of a mechanism for void growth in Li anodes. *Extreme Mech. Lett.* **46**, 101307.

Sargent P.M., Ashby, M.F., 1984. Deformation mechanism maps for alkali metals. *Scripta Mettal*. **18**, 145-150.

Schmidt, R.D., Sakamoto, J., 2016. In-situ, non-destructive acoustic characterization of solid-state electrolyte cells. *J. Power Sources* **324**, 126–133.

Seeger, A., Haasen, P., 1958. Density changes of crystals containing dislocations. *Phil. Mag. A* **3:29**, 470-475.

Sharafi, A., Kazyak, E., Davis, A.L., Yu, S., Thompson, T., Siegel, D.J., Dasgupta, N.P., Sakamoto, J., 2017a. Surface chemistry mechanism of ultra-low interfacial resistance in the solid-state electrolyte Li7La3Zr2O12. *Chem. Mater.* **29**, 7961-7968.

Sharafi, A., Haslam, C.G., Kerns, R.D., Wolfenstine, J., Sakamoto, J., 2017b. Controlling and correlating the effect of grain size with the mechanical and electrochemical properties of $Li_7La_3Zr_2O_{12}$ solid-state electrolyte. *J Mater. Chem A* **5**, 21491.

Shishvan, S.S., Fleck, N.A., McMeeking, R.M., Deshpande, V.S., 2020a. Dendrites as climbing dislocations in ceramic electrolytes: Initiation of growth. *J. Power Sources* **456**, 227989.

Shishvan, S.S., Fleck, N.A., McMeeking, R.M., Deshpande, V.S., 2020b. Growth rate of lithium filaments in ceramic electrolytes. *Acta Mater.* **196**, 444-455.

Shishvan, S.S., Fleck, N.A., Deshpande, V.S., 2021. The initiation of void growth during stripping of Li electrodes in solid electrolyte cells. *J. Power Sources* **488**, 229437.

Takada, K., 2013. Progress and prospective of solid-state lithium batteries. *Acta Mater.* **61**, 759–770.

Wang, M.J., Choudhury, R., Sakamoto, J., 2019. Characterizing the Li-solid-electrolyte interface dynamics as a function of stack pressure and current density. *Joule* **3**, 2165–2178.

Wang, M.J., Kazyak, E., Dasgupta, N.P., Sakamoto, J., 2021. Transitioning solid-state batteries from lab to market: Linking electro-chemo-mechanics with practical considerations. *Joule* **16**, 1371–1390.

Weertman, J., 1968. Dislocation climb theory of steady-state creep. *Trans. Am. Soc. Met.* **61**, 681-694.
Xu, C., Ahmad, Z., Aryanfar, A., Viswanathan, V., Greer, J.R., 2017. Enhanced strength and temperature dependence of mechanical properties of Li at small scales and its implications for Li metal anodes. *Proc. Natl. Acad. Sci. U.S.A.* **114**, 57–61.
Yan, H., Tantratian, K., Ellwood, K., Harrison, E.T., Nichols, M., Cui, X., Chen, L., 2022. How does the creep stress regulate void formation at the lithium-solid electrolyte interface during stripping? *Adv. Energy Mater.* **12**, 21022833.
Zhang, X., Wang, Q.J., Harrison, K.L., Roberts, S.A., Harris, S.J., 2020. Pressure-driven interface evolution in solid- state lithium metal batteries. *Cell Rep. Phys. Sci.* **1**, 100012.
Zhao, Y., Wang, R. Martinez-Paneda, E., 2022. A phase field electro-chemo-mechanical formulation for predicting void evolution at the Li–electrolyte interface in all-solid-state batteries. J Mech. Phys. Solids **167**, 104999.